

***In Vivo* Detection of Rat Colorectal Cancers by using a Dual-Wavelength Excitation Method**

**Kiichiro Miyawaki^{1,2,*}, Yoshinori Harada^{1,*}, Naoki Wakabayashi⁵,
Katsuichi Imaizumi^{1,4}, Noriaki Koizumi^{1,3}, Keimei Nakano², Yoshihisa Yamaoka¹,
Ping Dai¹, Yoshito Itoh² and Tetsuro Takamatsu¹**

¹Department of Pathology and Cell Regulation, Kyoto Prefectural University of Medicine Graduate School of Medical Science, ²Department of Gastroenterology and Hepatology, Kyoto Prefectural University of Medicine Graduate School of Medical Science, ³Division of Digestive Surgery, Department of Surgery, Kyoto Prefectural University of Medicine Graduate School of Medical Science, Kyoto 602–8566, Japan, ⁴Endoscopic Technology Department, Olympus Medical Systems Corp., Tokyo, Japan and ⁵Department of Gastroenterology and Hepatology, Otsu Municipal Hospital, Otsu 520–0804, Japan

Received August 6, 2014; accepted August 27, 2014; published online October 23, 2014

Hypoxia is a characteristic feature of solid neoplasms, and insufficient oxygen supply increases cellular nicotinamide adenine dinucleotide (NADH) fluorescence, which is a main component of autofluorescence of the colorectal mucosa. We investigated whether a dual-wavelength excitation method which is optimized for sensing mucosal NADH fluorescence could be applicable to the detection of rat colorectal cancers *in vivo*. Rat colorectal adenocarcinomas were studied by using fluorescence stereomicroscopy. After autofluorescence images at 470 nm irradiated with dual-wavelength excitation at 365 nm ($F_{365\text{ex}}$) and 405 nm ($F_{405\text{ex}}$) were acquired, ratio images were produced by dividing $F_{365\text{ex}}$ by $F_{405\text{ex}}$. The excitation-emission wavelength pairs in $F_{365\text{ex}}$ and $F_{405\text{ex}}$ were adjusted for acquisition of NADH fluorescence and reference fluorescence. Based on observations from the luminal surface *in vivo*, $F_{365\text{ex}}/F_{405\text{ex}}$ ratio images indicated a 1.57-fold higher signal value in the cancers than in the surrounding normal mucosa. The signal values in $F_{365\text{ex}}/F_{405\text{ex}}$ ratio images were less mutually related with the hemoglobin concentration index. Small adenocarcinomas (less than 4 mm) could be detected on $F_{365\text{ex}}/F_{405\text{ex}}$ ratio images. The results showed that NADH fluorescence measurement with little interference from tissue hemoglobin is efficient for visualizing rat colorectal cancers *in vivo*, suggesting that the dual-wavelength excitation method has potential for label-free endoscopic detection of diminutive colorectal neoplasms.

Key words: colorectal cancer, detection, fluorescence, *in vivo*, nicotinamide adenine dinucleotide

I. Introduction

Hypoxia is characteristic of primary solid neoplasms [12, 22]. Under hypoxic conditions, insufficient oxygen

supply introduces changes of the redox ratios of metabolism-related cellular fluorophores, such as nicotinamide adenine dinucleotide (NADH). It is reported that fluorescence of NADH is increased in hypoxic cells [13, 14]. Epithelial cells in the colorectal mucosa abundantly contain NADH [5, 13, 15, 16, 20, 21]. Change in mucosal autofluorescence in the process of neoplastic transformation may be useful in detecting diminutive epithelial neoplasms in the colorectum.

We have previously reported that adenomatous

*These authors contributed equally to this work.

Correspondence to: Tetsuro Takamatsu, Department of Pathology and Cell Regulation, Kyoto Prefectural University of Medicine Graduate School of Medical Science, 465 Kajii-cho Hirokoji Kawaramachi, Kamigyo-ku, Kyoto 602–8566, Japan. E-mail: ttakam@koto.kpu-m.ac.jp

mucosa could be distinguished from normal mucosa in endoscopically-resected *ex-vivo* human colorectal specimens by detecting alteration of NADH fluorescence in the mucosa [6]. In that study, we developed a dual-wavelength excitation method to evaluate NADH fluorescence in colorectal adenomatous mucosa without apparent reliance on tissue hemoglobin. After autofluorescence images at 470 nm irradiated with dual-wavelength excitation at 365 nm ($F_{365\text{ex}}$) and 405 nm ($F_{405\text{ex}}$) were serially obtained, $F_{365\text{ex}}/F_{405\text{ex}}$ ratio images were created. The excitation-emission wavelength pairs in $F_{365\text{ex}}$ and $F_{405\text{ex}}$ were designed to acquire NADH fluorescence and reference fluorescence. $F_{365\text{ex}}/F_{405\text{ex}}$ ratio images made clearly visible diminutive colorectal adenomas without interference from gross morphology or changes of vascularization in endoscopic mucosal resection (EMR) specimens.

It has not been demonstrated, however, whether the dual-wavelength excitation method is also effective in detecting tumors *in vivo* before excision. The aim of our present study was to examine whether the dual-wavelength excitation method could be applicable for *in-vivo* detection of rat colorectal cancers. Since the method is postulated to detect alterations of metabolic changes in the mucosal layer, it is preferable to precisely study specimens under *in-vivo* conditions. Furthermore, our previous study used EMR specimens to verify the feasibility of the method. It seems to be important to examine bowel specimens consisting of all layers of the wall, since the previous study failed to absolutely exclude the possibility that this method is influenced by autofluorescence emitted from submucosal collagen. The results showed that the dual-wavelength excitation method was applicable to *in-vivo* detection of diminutive colorectal cancers in rats.

II. Materials and Methods

Experimental colorectal tumor model

A preclinical rat model of azoxymethane (AOM)-induced colorectal tumors was used for the experiments. The induction of colorectal tumors was carried out according to previously reported protocols [10, 18]. Briefly, six-week-old male F344 rats were subcutaneously injected with AOM (Sigma Chemical Co., St Louis, MO, USA) in sterile saline at a dose of 15 mg/kg of body weight once a week for 3 weeks. The rats were regularly fed after injection of AOM. After the sixth month following the beginning of AOM treatment, screening examinations of the descending colon and rectum by endoscopy (BF TYPE 3C40; Olympus, Tokyo, Japan) were performed for the assessment of the presence or absence of tumors. In the presence of tumors, the tumor-bearing rats were subjected to experiments. Tumors of the descending colon and rectum were used for the subsequent analysis. All experimental procedures were approved by the Animal Care Committee of Kyoto Prefectural University of Medicine.

Sample preparation

In *ex-vivo* studies, the tumor-bearing rats were deeply anesthetized and their induced colorectal tumors with the surrounding non-tumorous tissues were quickly but carefully enucleated so as to prevent congestion and hypoxia. To minimize metabolic disintegration after resection, all samples were immediately immersed in physiologic saline at 4°C. In the cross-sectional study, colorectal tumors with surrounding non-tumor tissues were cut into slices with 1-mm-thickness and washed in physiologic saline. Cross-sectional specimens were prepared after acquisition of mucosal surface fluorescence images. The specimens were placed on a thermo plate kept at 3°C during experiments to keep them wet and fresh. All experiments were performed within 1 hour of excision.

In *in-vivo* experiments, the anesthetized rats were intubated with plastic tubes (outside diameter, 1.7 mm), and placed in the supine position. The intubated rats were artificially ventilated with room air. After abdominal midline incision, the anterior walls of the descending colon and rectum were cut open longitudinally with an electrosurgical knife. The exposed colorectal lumen was washed with saline at 37°C, and was scanned for colorectal tumors under white light imaging. The recognized colorectal tumor areas were then analyzed by a fluorescence stereomicroscopic system. The ventilated rats were placed on the thermo plate kept at 37°C during the experiment.

Microscopic imaging

A fluorescence stereomicroscopic imaging system previously described [6] was also used, with some modifications for this study. Briefly, the system for microscopic imaging consisted of a stereozoom microscope (SZX12; Olympus) equipped with a monochrome CCD camera (ORCA-ER; Hamamatsu Photonics, Hamamatsu, Japan), a mercury lamp (U-LH100HG; Olympus), an objective lens (DF PLAPO 1.2× PF2; Olympus), and a thermo plate (MATS-555S; Tokai Hit, Fujinomiya, Japan). A halogen lamp (LG-PS2; Olympus) and a color CCD digital camera (DP71; Olympus) were also equipped with the microscope to examine the structure of the samples, and 365-nm and 405-nm band-pass filters (D365/10× and D405/20×; Chroma Technology, Rockingham, Vermont) were used for 365 nm and 405 nm excitations, respectively. A 470-nm band-pass filter (D470/40m; Chroma) was used as an emission filter. A 610-nm band-pass filter (610DF20; Omega Optical, Brattleboro, Vt) and a 550-nm band-pass filter (HQ550/20×; Chroma) were used to acquire reflected images. Autofluorescence images at 470 nm illuminated with dual-wavelength excitation light at 365 nm ($F_{365\text{ex}}$) and 405 nm ($F_{405\text{ex}}$), and reflection images at 550 nm (R_{550}) and 610 nm (R_{610}), were taken by using the monochrome CCD. Dark current images measured without incoming lights were subtracted from measured fluorescence and reflection images for analysis.

Image analysis

Image analysis was performed as described previously [6] with some modifications. Briefly, Image J software (National Institutes of Health, Bethesda, Maryland) was used for analysis. After acquisition of F_{365ex} and F_{405ex} , ratio images were produced by dividing F_{365ex} by F_{405ex} . Signal intensities of autofluorescence and reflected light were evaluated from the images obtained by the monochrome CCD. Regions of interests (ROIs) were set over neoplastic sites and neighboring normal mucosal sites as assessed based on pathological features of the samples. Average pixel or ratio values of ROIs were reckoned using Image J. Bias of the monochrome CCD and variant exposure time were compensated prior to evaluation of pixel values. Ratios between signal intensities in tumorous regions and normal regions in F_{365ex} (T/N ratio in F_{365ex}), F_{405ex} (T/N ratio in F_{405ex}), and F_{365ex}/F_{405ex} ratio images (T/N ratio in F_{365ex}/F_{405ex}) were calculated. The sizes of tumors were defined by their maximum diameter measured from the color CCD images. $\text{Log}(R_{610}/R_{550})$ was adopted as a value for determining the amount of tissue hemoglobin, because the logarithm of the ratio of red reflectance to green reflectance is known as an estimating value for the tissue hemoglobin content [9, 19].

Histopathology

All of the tumor samples were subjected to pathologic examination after formalin fixation and paraffin embedding. Cross sections of 4 μm thickness were stained with hematoxylin-eosin (H&E). A pathologist conducted histopathological diagnosis without knowing the results of the fluorescence imaging.

Statistical analysis

The calculated signal intensity ratios between tumorous mucosa and normal mucosa were compared with 1.0 using a one-sample t-test. A probability value of less than 0.05 was considered significant. Data are given as means \pm standard deviations.

III. Results

Histopathology

A total of 21 AOM-induced colorectal tumors from 21 rats were included in this study. All of the tumor lesions were recognized as protruding lesions, and diagnosed as tubular adenocarcinomas. The sizes of the lesions ranged from 2.0 to 9.0 mm (average, 5.15 mm).

Dual-wavelength excitation imaging in colorectal cross-sections

Firstly, autofluorescence from the mucosal layer was observed in cross-sections of rat colorectal specimens ($n=10$: 10 cross-sections from 10 tumor tissues with surrounding non-tumor tissues) under the stereomicroscope. Stereomicroscopic and histologic images in a representative

cross-section of a colorectal adenocarcinoma are shown in Figure 1A–D. In F_{365ex} and F_{405ex} , it is difficult to identify obviously tumorous mucosa on the basis of fluorescence intensity, because the differences of fluorescence intensity between tumorous mucosa and normal mucosa are small (Fig. 1B and C). However, the ratio images of F_{365ex}/F_{405ex} showed tumorous lesions in accordance with the histological picture, as shown in Figure 1A and 1D. To quantitatively analyze the fluorescence of tumorous and normal mucosa on cross-sectional observation, we examined the T/N ratios in F_{365ex} , F_{405ex} , and F_{365ex}/F_{405ex} images (Fig. 1E). The average T/N ratio in F_{365ex} was more than 1.0 (1.40 ± 0.073 , $p < 0.01$), and that in F_{405ex} was less than 1.0 (0.81 ± 0.13 , $p < 0.01$). There were still a few cases observed in which lesions were difficult to differentiate from normal areas owing to the small difference between the T/N ratios and 1.0 in the case of F_{405ex} . The average T/N ratio in F_{365ex}/F_{405ex} demonstrated apparent increase (1.55 ± 0.12 , $p < 0.001$), and all of the analyzed adenocarcinomas could be detected clearly using T/N ratio in F_{365ex}/F_{405ex} .

Dual-wavelength excitation imaging from luminal surface in ex-vivo and in-vivo colorectums

We examined whether the dual-wavelength excitation method is suitable for tumor detection from the luminal surface. Representative images of an *ex-vivo* specimen of adenocarcinoma observed from the luminal surface are shown in Figure 2A–E. In the observation from this surface, the tumorous lesion was clearly identified on the ratio images of F_{365ex}/F_{405ex} (Fig. 2E). Figure 2F shows the quantitative results for T/N ratios in F_{365ex} , F_{405ex} , and F_{365ex}/F_{405ex} when *ex-vivo* specimens were observed from the luminal surface ($n=10$: 10 tumors with surrounding non-tumor tissues from 10 rats). The average T/N ratios in both F_{365ex} and F_{405ex} were less than 1.0 (F_{365ex} : 0.90 ± 0.22 ; F_{405ex} : 0.60 ± 0.22). On the other hand, the average T/N ratio in F_{365ex}/F_{405ex} demonstrated significant increase (1.62 ± 0.20 , $p < 0.001$), and all adenocarcinomas analyzed could be detected using T/N ratio in F_{365ex}/F_{405ex} .

Then, we examined whether the method is also effective for tumor detection from the luminal surface in *in-vivo* samples ($n=11$: 11 tumors in 11 rats). Representative images of an *in-vivo* sample of adenocarcinoma observed from the luminal surface are shown in Figure 3A–C. The tumor lesion was clearly identified in the F_{365ex}/F_{405ex} image (Fig. 3C). The quantitative results of the T/N ratios in F_{365ex} , F_{405ex} , and F_{365ex}/F_{405ex} images are shown in Figure 3D. The average T/N ratios in both F_{365ex} and F_{405ex} were less than 1.0 (F_{365ex} : 0.89 ± 0.48 ; F_{405ex} : 0.62 ± 0.34). In contrast, the average T/N ratio in F_{365ex}/F_{405ex} was 1.57 ± 0.28 ($p < 0.01$) (Fig. 3D), and all of the samples analyzed were also detectable using T/N ratio in F_{365ex}/F_{405ex} .

Influence of hemoglobin concentration on autofluorescence intensity in-vivo

To analyze the influence of blood volume on tissue

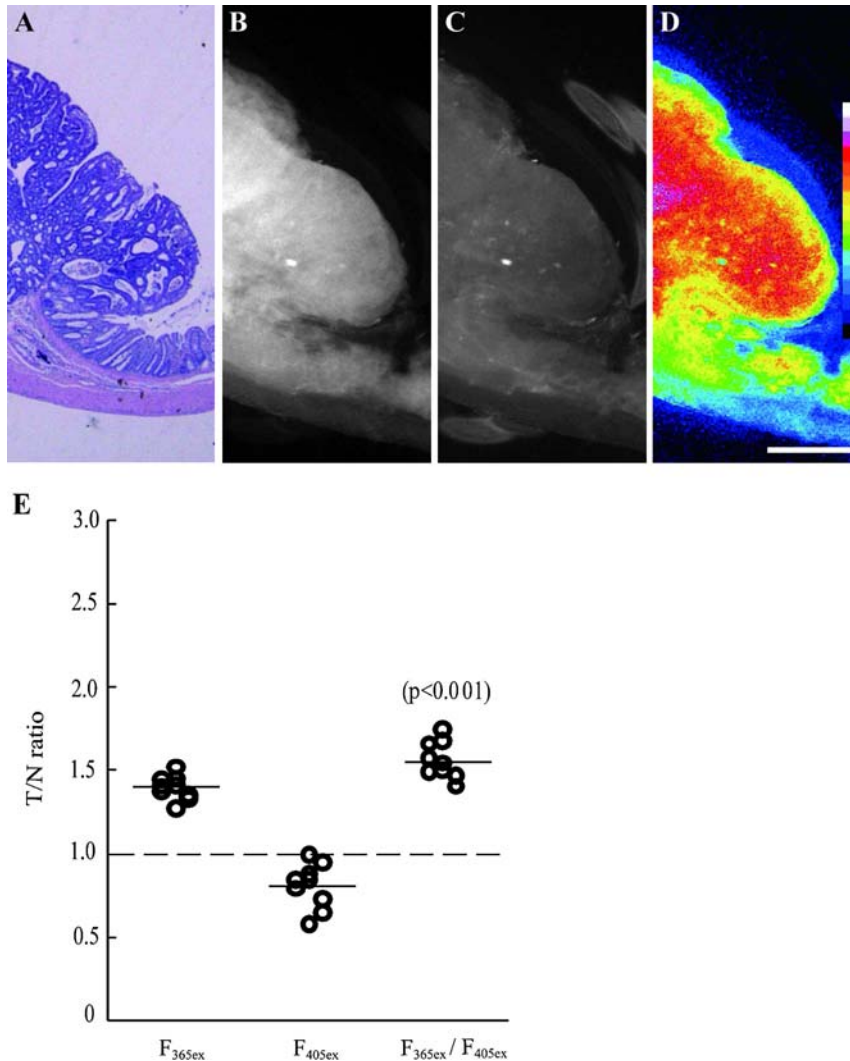


Fig. 1. Dual-wavelength excitation method can clearly distinguish cancerous mucosa from non-cancerous mucosa in sliced colorectal cross-sections. Representative images of a sliced cross-section of colorectal adenocarcinoma are shown (A–D). H&E-stained image (A) revealed histology of adenocarcinoma. Autofluorescence images [(B) (F_{365ex} : fluorescence at 470 nm with 365-nm excitation) and (C) (F_{405ex} : fluorescence at 470 nm with 405-nm excitation)] and a pseudocolor ratio image (D) acquired by dividing F_{365ex} by F_{405ex} , are presented. Different colors in the pseudocolor ratio image (D) indicate different ratios as shown by the inserted color bars. Scatter plots for ratios between signal intensities in tumorous regions and normal regions (T/N ratios) in F_{365ex} , F_{405ex} , and F_{365ex}/F_{405ex} are shown in E. Bar=1 mm (D). The short horizontal lines in E show average values.

autofluorescence *in vivo*, signal values of non-tumoral mucosal regions in F_{365ex} , F_{405ex} , and F_{365ex}/F_{405ex} ratio images were compared with $\log(R_{610}/R_{550})$, an index of hemoglobin concentration: R_{550} and R_{610} represent reflection intensities at 550 nm and 610 nm, respectively ($n=12$: 12 regions in 6 rats). The signal intensities in F_{365ex} and F_{405ex} tended to decrease as $\log(R_{610}/R_{550})$ increased (Fig. 4A and B). The slopes of the linear fitting curves in F_{365ex} and F_{405ex} were -2.1 and -3.2 , respectively. However, the signal values in F_{365ex}/F_{405ex} ratio images were less mutually related with $\log(R_{610}/R_{550})$ (Fig. 4C). The slope of the linear fitting curve in F_{365ex}/F_{405ex} (-0.7) was smaller than those in F_{365ex} and F_{405ex} . The results showed that the signal intensities in F_{365ex}/F_{405ex} ratio images were less affected by blood volume contained in *in-vivo* tissues.

Relation between T/N ratio in F_{365ex}/F_{405ex} and sizes of adenocarcinomas

The T/N ratio in F_{365ex}/F_{405ex} on luminal observation was compared with the sizes of the neoplasms to evaluate its validity in visualizing small neoplasms. Figure 5 shows the relation between T/N ratio in F_{365ex}/F_{405ex} and maximum diameter of both *ex-vivo* (black dots) and *in-vivo* (white dots) adenocarcinomas. The results showed that small adenocarcinomas less than 4 mm in diameter were well-discriminated in F_{365ex}/F_{405ex} ratio images even in *in-vivo* experiments.

IV. Discussion

In this study, we examined the efficacy of the dual-

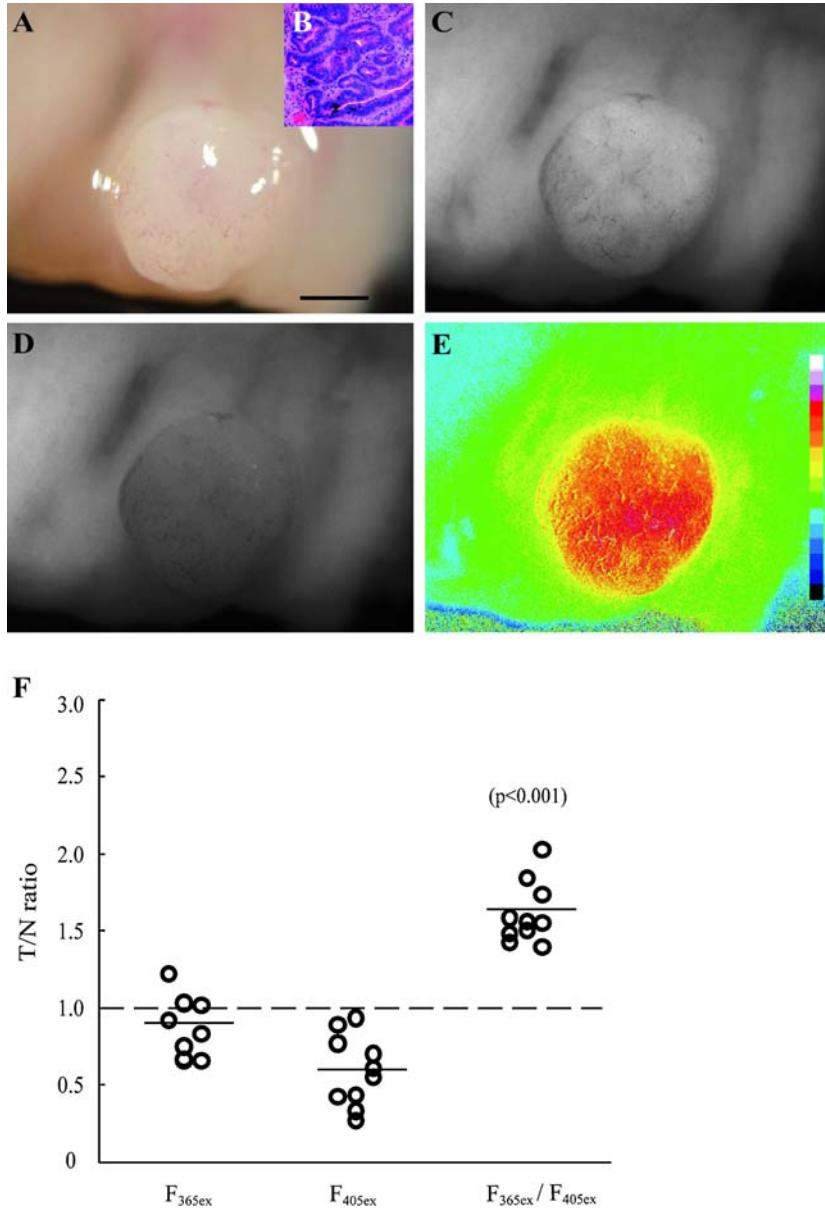


Fig. 2. *Ex-vivo* detection of colorectal adenocarcinomas from luminal surface by using the dual-wavelength excitation method. Representative images of an *ex-vivo* colorectal adenocarcinoma are shown (A–E): A white-light image (A), an H&E-stained image (B), autofluorescence images (C, F_{365ex}; D, F_{405ex}), and a pseudo-color ratio image (E) obtained by dividing F_{365ex} by F_{405ex}. Different colors in E indicate different ratios as shown by the inserted color bars. Bar=1 mm (A). Scatter plots for the T/N ratios of F_{365ex}, F_{405ex}, and F_{365ex}/F_{405ex} in *ex-vivo* samples are shown in F. The short horizontal lines show average values.

wavelength excitation method to detect rat colorectal adenocarcinomas *in vivo*. To address this issue, we firstly elucidated the mucosal fluorescence intensities in cross-sections of colorectal cancers. Cross-sectional samples were used to analyze the neoplastic/non-neoplastic mucosal fluorescence without the overlay of submucosal fluorescence or the influence of mucosal thickness. By using the dual-wavelength excitation method, we found that all of the cancerous mucosae examined could be distinguished from non-cancerous mucosae in the cross-sectional samples.

It is important to examine whether the dual-

wavelength excitation method can be applied for cancer detection from the luminal surface in consideration of the possible future application to endoscopic examination. The colorectal wall constitutes a multilayered structure, and in addition to the metabolic fluorophores mainly distributed in the mucosal layers, other bright endogenous fluorophores, such as collagen and elastin, are contained in the submucosal layers in the colorectum [7, 21]. The results showed that the dual-wavelength excitation method was also effective for cancer detection under observation from the luminal surface under not only *ex-vivo* but also *in-vivo*

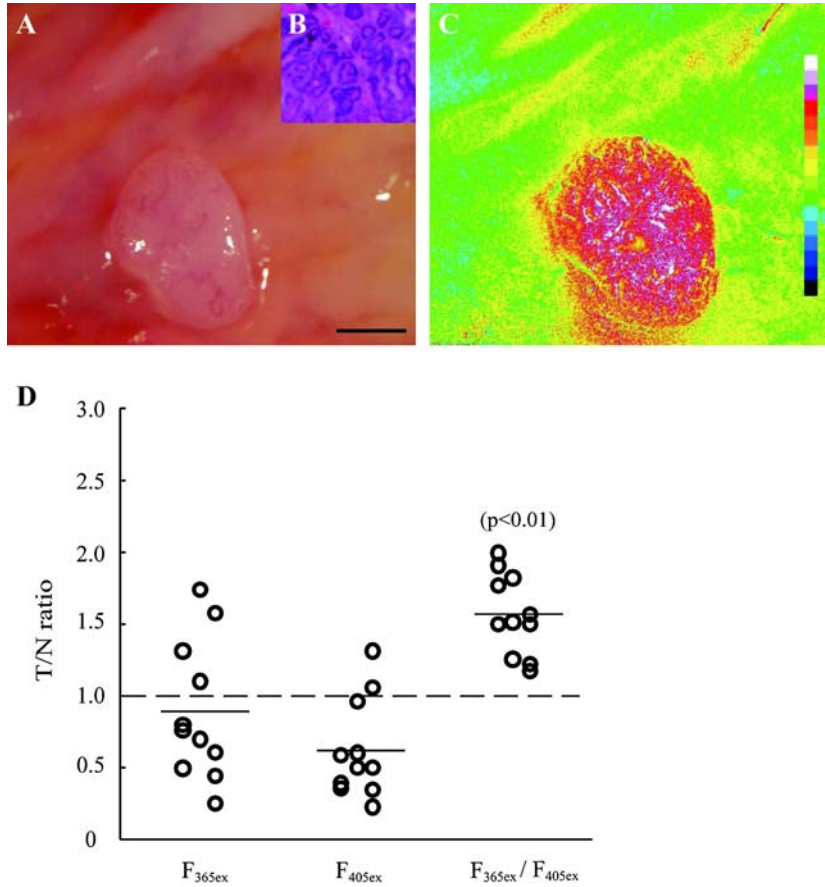


Fig. 3. Dual-wavelength excitation method can identify cancerous lesion in the observation from the luminal surface *in-vivo*. Representative images of a colorectal adenocarcinoma are shown (A–C): A white-light image (A), an H&E-stained image (B), and a pseudo-color ratio image (C) obtained by dividing F_{365ex} by F_{405ex} . Different colors in C represent different ratios as indicated by the inserted color bars. Bar=1 mm (A). Scatter plots for the T/N ratios of F_{365ex} , F_{405ex} , and F_{365ex}/F_{405ex} in *in-vivo* samples are shown in D. The short horizontal lines show average values.

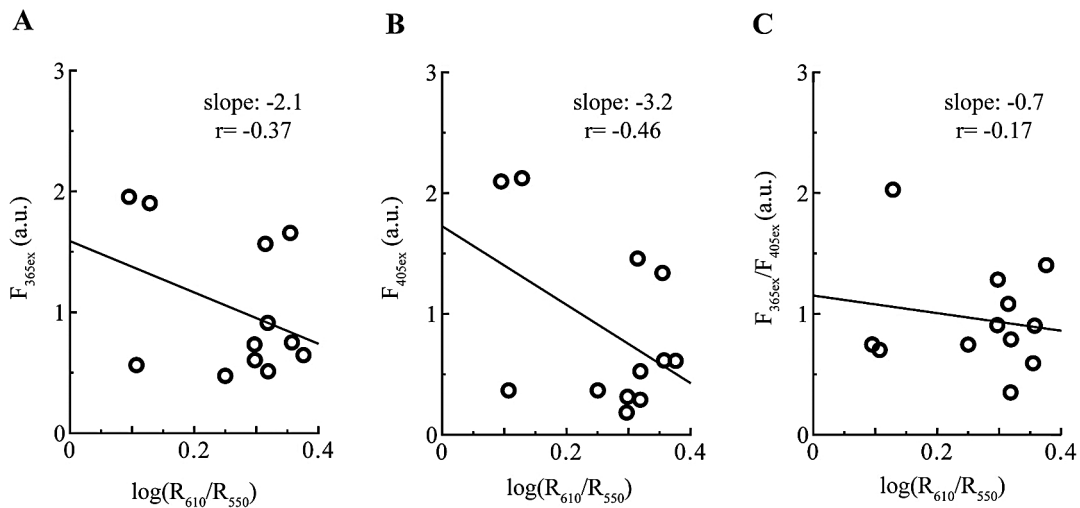


Fig. 4. Association between fluorescence intensity and hemoglobin concentration *in-vivo*. The relation of F_{365ex} signal intensities to $\log(R_{610}/R_{550})$ (A), F_{405ex} signal intensities to $\log(R_{610}/R_{550})$ (B), and F_{365ex}/F_{405ex} signal intensities to $\log(R_{610}/R_{550})$ (C) were measured for *in-vivo* specimens on luminal observation. No significant correlation between F_{365ex}/F_{405ex} and $\log(R_{610}/R_{550})$ [r (correlation coefficient) = -0.17 (C)] was observed. R_{610} and R_{550} represent reflection intensities at 610 nm and 550 nm, respectively. a.u., arbitrary units.

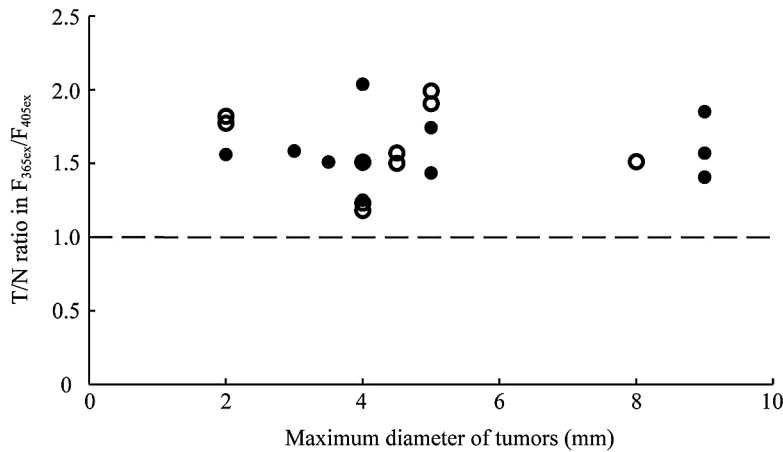


Fig. 5. Relation between T/N ratios in F_{365ex}/F_{405ex} when observed from the luminal surface and tumor size. T/N ratio in F_{365ex}/F_{405ex} and the sizes of tumors were compared. Adenocarcinomas less than 4 mm in diameter demonstrated high T/N ratios in F_{365ex}/F_{405ex} , as did large adenocarcinomas. Black and white dots indicate the results of *ex-vivo* (n=10) and *in-vivo* (n=11) samples.

conditions. Fluorescence signals of the mucosa were not overwhelmed by those of the submucosa even under the *in-vivo* condition.

Our results demonstrated that the average T/N ratio in F_{365ex} , which was acquired by a single-wavelength excitation light, was more than 1.0 in *ex-vivo* cross-sectional specimens in a reflection of the strong NADH fluorescence intensity in cancerous lesions (Fig. 1E). However, the average T/N ratio in F_{365ex} in *in-vivo* specimens was less than 1.0, as shown in Figure 3D. This may be partly because the *ex-vivo* specimens seemed to have a lower blood content than the *in-vivo* specimens: In the *ex-vivo* specimens cut into slices with 1-mm-thickness, blood in the tissues was considered to have oozed out in physiologic saline during the specimen-making process, and blood hemoglobin absorbs both excitation and emission light of NADH [4, 6]. In the dual-wavelength excitation method, the reference fluorescence could compensate for the absorption effect of hemoglobin. Indeed, the signal intensities in F_{365ex}/F_{405ex} ratio images were less affected by blood hemoglobin in the *in-vivo* samples (Fig. 4C). Therefore, the method seemed to be suitable for *in-vivo* detection of cancerous lesions based on NADH fluorescence. As for the reference fluorescence, the main fluorophores responsible for the reference fluorescence may be flavoproteins [5, 6, 21]. Flavoprotein fluorescence is reported to show behavior inverse to NADH fluorescence in cells [11, 17, 21]. No effects on T/N ratio in F_{365ex}/F_{405ex} ratio images from the tumor site or degree of tumor differentiation were apparent in this study.

The ratio imaging using two excitation lights is useful for shading correction on three-dimensional objects such as hollow organs. Structures near the light source or in a plane perpendicular to the light axis tend to show strong signals. Conversely, structures far from the light source or in a plane parallel to the light axis tend to show dark signals. Such uneven illumination using a single excitation light in the gastrointestinal lumen can possibly lead to false detec-

tion of colorectal tumors. Our dual-wavelength excitation method can compensate for the effect of uneven illumination by dividing two images obtained with two excitation lights, as shown in Figures 1, 2, and 3. Therefore, the dual-wavelength excitation method may have potential for future development of a new device for automated identification of colorectal tumors.

Among the limitations of this study, firstly, we studied a rat model of colorectal cancers, not human colorectal cancers. It seems to be difficult to precisely study autofluorescence characteristics by using surgically-resected human colorectal cancer samples or human cancer specimens from endoscopic submucosal dissection, especially when focusing on metabolic fluorophores, because such samples, excised by relatively prolonged invasive treatments with hemostasis, are commonly in a severely ischemic state, i.e., hypoxic state. Secondly, we only found the histology of tubular adenocarcinoma in this experiment, and we studied neither colorectal cancer specimens coexistent with inflammatory bowel disease nor aberrant crypt foci. Future *in-vivo* research on human tumors with various histological types or with inflammatory bowel diseases is needed to verify the efficacy of this method in more depth. Thirdly, flat-type neoplastic lesions were not included in this study, although this method seems to have a potential to distinguish flat-type diminutive neoplastic lesions as discussed in the previous study [6]. In this study, we examined cross-sections of rat colorectal adenocarcinomas in order to demonstrate that this method was little-affected by the configuration of the specimens. Finally, the UVA light illumination has a potential to be harmful to the tissues. However, an optical implement to survey cervical neoplasms utilizing a UV light has been clinically applied [1, 2, 8]. Although it necessitates careful estimation of the use of UVA light, the brief use of UVA light at around 400 nm could be utilized on clinical inspection [3].

In our present study, we examined the efficacy of the

dual-wavelength excitation method to detect rat colorectal adenocarcinomas *in vivo*. Although *in-vivo* investigation using human colorectal neoplasms is indeed necessary, our results suggest the potential of the dual-wavelength excitation method as a label-free imaging technique of detecting diminutive neoplasms, which may be contributory to improving the usefulness of autofluorescence endoscopy of digestive tracts.

V. Abbreviations

AOM, azoxymethane; EMR, endoscopic mucosal resection; H&E, hematoxylin-eosin; NADH, nicotinamide adenine dinucleotide; ROI, regions of interest

VI. Acknowledgments

We thank Mrs. T. Okuda and T. Kawamura, Department of Pathology and Cell Regulation, for assistance in histological examination. This work was partly supported by the Nanomedicine Device Development Project of the New Energy and Industrial Technology Development Organization (NEDO), a Grant-in-Aid for Scientific Research (KAKENHI) and Olympus Medical Systems Corp.

VII. References

- Alvarez, R. D. and Wright, T. C. (2007) Effective cervical neoplasia detection with a novel optical detection system: a randomized trial. *Gynecol. Oncol.* 104; 281–289.
- Alvarez, R. D. and Wright, T. C., Jr. (2007) Increased detection of high-grade cervical intraepithelial neoplasia utilizing an optical detection system as an adjunct to colposcopy. *Gynecol. Oncol.* 106; 23–28.
- Brookner, C. K., Agrawal, A., Trujillo, E. V., Mitchell, M. F. and Richards-Kortum, R. R. (1997) Safety analysis: relative risks of ultraviolet exposure from fluorescence spectroscopy and colposcopy are comparable. *Photochem. Photobiol.* 65; 1020–1025.
- Chance, B., Cohen, P., Jobsis, F. and Schoener, B. (1962) Intracellular oxidation-reduction states *in vivo*. *Science* 137; 499–508.
- Hall, C. L. and Kamin, H. (1975) The purification and some properties of electron transfer flavoprotein and general fatty acyl coenzyme A dehydrogenase from pig liver mitochondria. *J. Biol. Chem.* 250; 3476–3486.
- Imaizumi, K., Harada, Y., Wakabayashi, N., Yamaoka, Y., Konishi, H., Dai, P., Tanaka, H. and Takamatsu, T. (2012) Dual-wavelength excitation of mucosal autofluorescence for precise detection of diminutive colonic adenomas. *Gastrointest. Endosc.* 75; 110–117.
- Izuishi, K., Tajiri, H., Fujii, T., Boku, N., Ohtsu, A., Ohnishi, T., Ryu, M., Kinoshita, T. and Yoshida, S. (1999) The histological basis of detection of adenoma and cancer in the colon by autofluorescence endoscopic imaging. *Endoscopy* 31; 511–516.
- Kendrick, J. E., Huh, W. K. and Alvarez, R. D. (2007) LUMA cervical imaging system. *Expert Rev. Med. Devices* 4; 121–129.
- Kim, G. H., Kim, K. B., Lim, E. K., Choi, S. H., Kim, T. O., Heo, J., Kang, D. H., Song, G. A., Cho, M. and Park, D. Y. (2006) Analysis of endoscopic electronic image of intramucosal gastric carcinoma using a software program for calculating hemoglobin index. *J. Korean Med. Sci.* 21; 1041–1047.
- Kobaek-Larsen, M., Thorup, I., Diederichsen, A., Fenger, C. and Hoitinga, M. R. (2000) Review of colorectal cancer and its metastases in rodent models: comparative aspects with those in humans. *Comp. Med.* 50; 16–26.
- Kuznetsov, A. V., Mayboroda, O., Kunz, D., Winkler, K., Schubert, W. and Kunz, W. S. (1998) Functional imaging of mitochondria in saponin-permeabilized mice muscle fibers. *J. Cell Biol.* 140; 1091–1099.
- Li, X. F., Carlin, S., Urano, M., Russell, J., Ling, C. C. and O'Donoghue, J. A. (2007) Visualization of hypoxia in microscopic tumors by immunofluorescent microscopy. *Cancer Res.* 67; 7646–7653.
- Mayevsky, A. and Chance, B. (1982) Intracellular oxidation-reduction state measured *in situ* by a multichannel fiber-optic surface fluorometer. *Science* 217; 537–540.
- Mayevsky, A. and Rogatsky, G. G. (2007) Mitochondrial function *in vivo* evaluated by NADH fluorescence: from animal models to human studies. *Am. J. Physiol. Cell Physiol.* 292; C615–640.
- Nakano, K., Harada, Y., Yamaoka, Y., Miyawaki, K., Wakabayashi, N., Imaizumi, K., Takaoka, H., Nakaoka, M. and Takamatsu, T. (2009) Analysis of rat colonic mucosal autofluorescence under excitation with UV/violet light. *IFMBE Proceedings* 25; 860–861.
- Nakano, K., Harada, Y., Yamaoka, Y., Miyawaki, K., Wakabayashi, N., Imaizumi, K., Takaoka, H., Nakaoka, M., Yoshikawa, T. and Takamatsu, T. (2013) Precise analysis of the autofluorescence characteristics of rat colon under UVA and violet light excitation. *Curr. Pharm. Biotechnol.* 14; 172–179.
- Skala, M. C., Ricking, K. M., Gendron-Fitzpatrick, A., Eickhoff, J., Eliceiri, K. W., White, J. G. and Ramanujam, N. (2007) *In vivo* multiphoton microscopy of NADH and FAD redox states, fluorescence lifetimes, and cellular morphology in precancerous epithelia. *Proc. Natl. Acad. Sci. U S A* 104; 19494–19499.
- Tanaka, T., Kohno, H., Shimada, R., Kagami, S., Yamaguchi, F., Kataoka, S., Ariga, T., Murakami, A., Koshimizu, K. and Ohigashi, H. (2000) Prevention of colonic aberrant crypt foci by dietary feeding of garcinol in male F344 rats. *Carcinogenesis* 21; 1183–1189.
- Tsuji, S., Sato, N., Kawano, S. and Kamada, T. (1988) Functional imaging for the analysis of the mucosal blood hemoglobin distribution using electronic endoscopy. *Gastrointest. Endosc.* 34; 332–336.
- Ueno, K., Kusunoki, Y., Imamura, F., Yoshimura, M., Yamamoto, S., Uchida, J. and Tsukamoto, Y. (2007) Clinical experience with autofluorescence imaging system in patients with lung cancers and precancerous lesions. *Respiration* 74; 304–308.
- Wu, Y. and Qu, J. Y. (2006) Autofluorescence spectroscopy of epithelial tissues. *J. Biomed. Opt.* 11; 054023.
- Zhong, H., De Marzo, A. M., Laughner, E., Lim, M., Hilton, D. A., Zagzag, D., Buechler, P., Isaacs, W. B., Semenza, G. L. and Simons, J. W. (1999) Overexpression of hypoxia-inducible factor 1 α in common human cancers and their metastases. *Cancer Res.* 59; 5830–5835.